Proc. Natl. Acad. Sci. USA
Vol. 86, pp. 711–715, January 1989
Neurobiology

Spatial-frequency organization in primate striate cortex

(cortical modules/multiple channels/cytochrome oxidase "blobs")

MARTIN S. SILVERMAN*, DAVID H. GROSOF, RUSSELL L. DE VALOIS, AND SYLVIA D. ELFAR

Department of Psychology and Neurobiology Group, University of California, Berkeley, CA 94720

Contributed by Russell L. De Valois, October 4, 1988

ABSTRACT **We measured the spatial-frequency tuning of cells at regular intervals along tangential probes through the monkey striate cortex and correlated the recording sites with the cortical cytochrome oxidase (CytOx) patterns to address three questions with regard to the cortical spatial-frequency organization. (*i*) Is there a periodic anatomical arrangement of cells tuned to different spatial-frequency ranges? We found there is, because the spatial-frequency tuning of cells along tangential probes changed systematically, varying from a low frequency to a middle range to high frequencies and back again repeatedly over distances of about 0.6–0.7 mm. (*ii*) Are there just two populations of cells, low-frequency and high-frequency units, at a given eccentricity (perhaps corresponding to the magno- and parvocellular geniculate pathways) or is there a continuum of spatial-frequency peaks? We found a continuum of peak tuning. Most cells are tuned to intermediate spatial frequencies and form a unimodal rather than a bimodal distribution of cell peaks. Furthermore, the cells with different peak frequencies were found to be continuously and smoothly distributed across a module. (*iii*) What is the relation between the physiological spatial-frequency organization and the regions of high CytOx concentration ("blobs")? We found a systematic correlation between the topographical variation in spatial-frequency tuning and the modular CytOx pattern, which also varied continuously in density. Low-frequency cells are at the center of the blobs, and cells tuned to increasingly higher spatial frequencies are at increasing radial distances.**

The primary transformation of visual information at the striate cortex level in cat and monkey appears to be the sharpening of the orientation and spatial-frequency tuning of cells (1–5). Retinal ganglion and lateral geniculate nucleus cells respond to a wide range of orientations and spatial frequencies, whereas striate cortex cells are usually much more narrowly tuned. In the striate cortex, most cells have both spatial frequency and orientation tuning and thus respond to only a limited two-dimensional spatial-frequency range, each acting in effect as a band-pass two-dimensional filter of patterns within a localized region of the visual field. Different cells within a cortical region respond to different two-dimensional frequency ranges, with the ensemble of cells presumably covering the whole three- to five-octave range of spatial frequencies visible at that eccentricity (5). This physiological evidence is in good agreement with considerable psychophysical evidence for the presence of multiple two-dimensional spatial-frequency channels underlying human spatial vision (6–9).

Early studies of the anatomical arrangement of cells in macaque striate cortex found evidence for a modular pattern to the cortical organization (10, 11). The cells within a slab of cortex ≈1–1.5 mm on a side all process the visual input from one small retinal region. Half of the cells within such a module receive their primary input from one eye, and the other half from the other eye. Within each half-module are found cells tuned to all of the different orientations in a systematic order. These early studies did not examine the spatial-frequency organization.

Staining the cortex for cytochrome oxidase (CytOx) reveals an anatomical pattern of CytOx-rich "blobs" (regions of high CytOx concentration) distributed across the whole striate cortex in a striking leopard-like pattern (12–14). CytOx blobs turn out to be systematically related to the columnar organization for ocular dominance, a single CytOx blob being at the center of each half-module (12, 15, 16).

We have studied (17, 18) the arrangement of different functional groups of cells within the cortex, using the 2-deoxy-D-[U-^{14}C]glucose (2-dG) technique and found a systematic spatial-frequency organization. Low spatial-frequency stimulation produced 2-dG uptake restricted to the CytOx blobs, whereas high-frequency stimulation produced uptake restricted to the interblobs. Middle spatial frequencies produced an essentially uniform pattern of activation in blobs and interblobs (CytOx-poor areas interspersed between blobs).

These 2-dG studies left certain unanswered questions, however, to which the present experiment is addressed. A principal question is whether there are more than just two classes of cells—those tuned to low spatial frequencies and those tuned to high ones—given that only two discrete anatomical patterns could be discerned in the 2-dG uptake. Such a bimodal spatial-frequency organization would appear quite unlikely, given the extensive psychophysical evidence for multiple (not just two) spatial-frequency channels, and is hardly demanded by the 2-dG evidence cited above, given the relatively poor spatial resolution of the technique. Nonetheless, a bimodal-frequency distribution is a possibility that must be considered, particularly since there is much recent evidence for two functionally separate projections through the visual system that are segregated at the lateral geniculate level into the magno- and the parvocellular laminae and in the striate cortex in the 4Cα and 4Cβ laminae. In addition, there is evidence that these two systems have somewhat different spatial-frequency tuning on the average. Thus, it is conceivable that the blob pattern seen with low-spatial-frequency stimulation reflects just magnocellular-related activity, and the high-frequency interblob pattern reflects parvocellular activity rather than a true multiple-spatial-frequency organization.

Given that cells with a variety of peak spatial frequencies occur within a striate region, a related question is whether these cells are arranged in a regular order or randomly distributed throughout the module. To examine these questions, we have turned to microelectrode recording, with its finer spatial resolution.

The publication costs of this article were defrayed in part by page charge payment. This article must therefore be hereby marked "*advertisement*" in accordance with 18 U.S.C. §1734 solely to indicate this fact.

Abbreviations: CytOx, cytochrome oxidase; 2-dG, 2-deoxy-D-[U-^{14}C]glucose; c/deg, cycles per degree; V1 and V2, visual areas 1 and 2.

*Present address: Central Institute for the Deaf, and Department of Anatomy and Neurobiology, Washington University School of Medicine, Saint Louis, MO 63110.

MATERIALS AND METHODS

We recorded from cells at regular sites along a long tangential probe through the striate cortex, quantitatively measuring the spatial-frequency tuning of the cells encountered at each recording locus. The recording techniques were similar to those described elsewhere (5, 19). The macaque monkey was held painlessly by a pedestal attached to the skull in a prior operation. Anesthesia was induced with ketamine, and the animal was maintained anesthetized throughout the experiment by continuous infusion of morphine (0.7–1 mg/kg of body weight per hr) supplemented by N_2O; eye movements were minimized by paralysis with pancuronium bromide (Pavulon). Contact lenses kept the eyes from drying, and appropriate lenses were placed before each eye to bring the experimental stimuli to a focus on the retina.

We used electrodes with longer than usual tips (15–25 μm) to sample a small group of cells at each recording site. The electrode was inserted at a very acute angle with respect to the cortical surface, just posterior to the lunate sulcus, close to the border of visual areas 1 and 2 (V1–V2 border). Thereby we were able to make tangential penetrations up to 3 mm through the upper layers of the cortex.

At the termination of the experiment, the opercula were removed and flattened (20). The cortex was then sectioned parallel to the electrode tracks at 40 μm, and the sections were treated for CytOx (21). Histological examination of the electrode tracks, of several small lesions made along each probe, and of the CytOx pattern in that and adjacent sections enabled us to localize each recording site with respect to the CytOx blobs. Densitometry along the electrode path allowed us to specify quantitatively the CytOx density at each recording site.

The stimuli consisted of luminance-varying achromatic grating patterns presented monocularly under computer control on a monitor located 114 cm from the animal. The receptive field was centered on the display by appropriate movement of the monitor and/or of the animal's head, which was held in a gimbal arrangement.

On the main probes, recordings were made every 100 μm along the electrode track. At each site, the preferred orientation and the ocular dominance of the unit(s) were first determined with hand-held stimuli. Then the spatial-frequency tuning was quantitatively measured with optimally oriented gratings of various spatial frequencies presented in a random order, drifting across the receptive field at 2–4 Hz. The computer analyzed the windowed spike discharge. We then advanced the electrode to the next recording site.

RESULTS

The retinotopic projection to the cortex is such that points on a ring at a given retinal eccentricity project onto a straight line running anterio-posteriorly across the operculum (22). Therefore, our electrode probes, directed posteriorly from the V1–V2 border, went through striate cortical regions all related to the same retinal eccentricity. [The slight, second-order deviation from this projection pattern (22) is insignificant for the distances our probes extended.] This approach has one additional advantage—namely, that it allows a long, almost exactly tangential probe: the curve of the cortex at the V1–V2 border (where it starts to dip into the lunate sulcus) allows the electrode to reach the cortex parallel to the surface of the subsequent (flat) extent of the operculum. Histological examination of our probes indicates that in fact they did stay within a pair of laminae throughout the 2.5- to 3-mm lengths of the tracks. The probes in the right hemisphere were all through the blobs and interblobs of the supragranular layers 2 and 3, and in the left hemisphere were through the blobs and interblobs of layers 5 and 6.

Our data are from four long penetrations, along two of which recordings were made every 100 μm. Those two probes (labeled P-L1 and P-R1), one on each hemisphere, passed through a cortical region 3° eccentric (a determination based on an examination of the opercula at the end of the experiment). Two additional probes (P-R2 and P-R3) were made parallel with and 1 mm to either side of P-R1, with less frequent samples.

Periodicity of Spatial-Frequency Peaks. The responses of the cell(s) at each recording locus to gratings of various spatial frequencies were plotted and curve fitted by eye to determine the peak spatial frequency at this locus. These peak values were then plotted as a function of distance along the probe. Fig. 1*C* shows the resulting data for probe L1. A key issue with respect to these data is whether the distribution of peak frequencies is periodic.

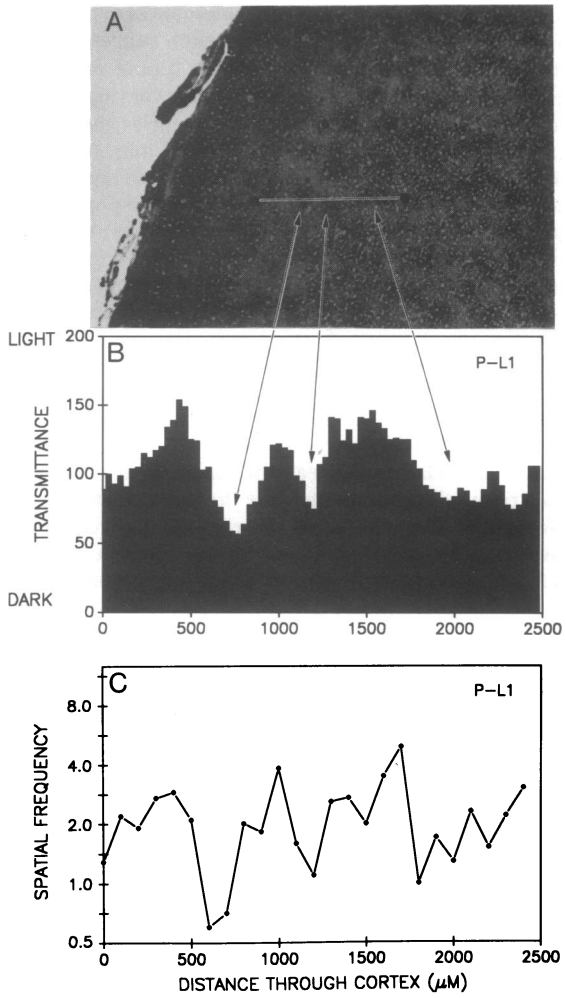

FIG. 1. Comparison of the CytOx pattern and spatial-frequency tuning of cells. (*A*) A CytOx-stained flat-mounted section through the left striate cortex in the plane of the electrode, showing the pattern of CytOx blobs. The location of the electrode track for P-L1 is marked with a line, along with the starting and end points over which the data were collected. (*B*) Densitometric measures along the electrode track marked in *A*. The values at each point are based on a moving average over a square block of nine adjacent pixels to reduce the effect of artifacts from blood vessels. Linear transmission values are plotted, and the arrows from *A* to *B* show the locations of the three blobs traversed by this track in relation to the densitometry. (*C*) A plot of the peak spatial-frequency tuning of units in cycles per degree (c/deg) recorded every 100 μm along the electrode track shown in *A*. It can be seen that the cells tuned to the lowest spatial frequencies are located in regions of high CytOx density (blobs), and those tuned to increasingly higher spatial frequencies are increasingly further from the blob centers.

It appears clear from a visual inspection of data shown in Fig. 1*C* (and of comparable plots for probes R1 and R3, to be seen in the dashed lines in Fig. 3 *B* and *C*) that the peak spatial-frequency tuning of cells does in fact vary periodically as one traverses the cortex. There are points with high-spatial frequency cells at about 400, 1000, 1700, and 2400 μm along track P-L1 and low-spatial-frequency cells at about 600, 1200, and 1800 μm. We tested this visual judgment by making a quantitative measure of the periodicity. We analyzed (Fourier analysis) the waveform shown in Fig. 1 and examined the power at different harmonics as a function of the data sequence length (by truncating the series or by padding it with the mean value). This, plus a harmonic regression to find the best-fitting sinusoid, showed that the data were periodic with a period of about 660 μm. The periods in the other probes were also found to be between 600 and 725 μm. To evaluate the significance of the largest peaks in the power spectrum, Fisher's test for periodicity (23, 24) was applied. The joint probability that both P-L1 and P-R1 would show such large peaks was $0.008 < P < 0.009$.

Only Two Populations of Cells? A second question is whether there are cells with many different preferred spatial frequencies distributed unimodally or whether there are only two classes of cells (those tuned to high spatial frequencies and those tuned to low ones, with perhaps some random scatter within each group). The earlier 2-dG experiments left us uncertain on this point because only two distinct patterns of selective 2-dG uptake (either on the CytOx blobs or off the blobs) could be seen with different spatial frequency stimulation.

A straightforward way of answering this question is to examine a histogram of the spatial-frequency peaks (see Fig. 2) where data are presented for each of the main probes, P-L1 and P-R1, and for all four probes together. In each subgraph it can be clearly seen that the cells range widely in their peak tuning and that the majority of cells are tuned to mid-spatial-frequencies. Thus, there is a unimodal distribution of peak tuning, not the bimodal distribution one would expect if there were only two cell types at a given eccentricity.

The decrease in average spatial-frequency-peak tuning with increasing eccentricity is an important factor that could confound an attempt to examine the range of tuning within a striate region. Note, however, that the data shown in Fig. 2 were all collected at a single eccentricity. Each of the individual probes went through cortical regions corresponding to a constant retinal eccentricity, so the top two histograms are not confounded with eccentricity. Furthermore, P-L1 and P-R1, although on different halves of the brain, were found to be at the same eccentricity, as determined by examining the recording sites on the two opercula at the termination of the experiment. P-R2 and P-R3 went through neighboring cortical modules from those traversed by P-R1, but the change in magnification factor from one module to the adjacent one is insignificant compared with the range of peak tuning. Therefore, one is justified in combining all of the data, as we have done in Fig. 2 *Bottom*. Note that the cells encountered in P-R1 were on average tuned to a higher spatial-frequency range than the others. This is related to the differing paths of the electrodes with respect to the centers of the cortical modules, as is discussed below.

Having pooled all data into a single histogram, we wanted to determine how likely it was for the distribution of Fig. 2 to have been drawn from a mixed distribution composed of about one-fifth (15) low-mean "blob" cells and the rest higher mean "interblob" cells. With a χ^2 goodness-of-fit criterion, we tried modeling the data as a mix of two component populations, distributed as either normal or γ (25). No sum of two normal populations fit the data. They could be fit by a sum of two γ distributions, but only if the two populations had similar modes (<2 c/deg apart) and the second (lower mean)

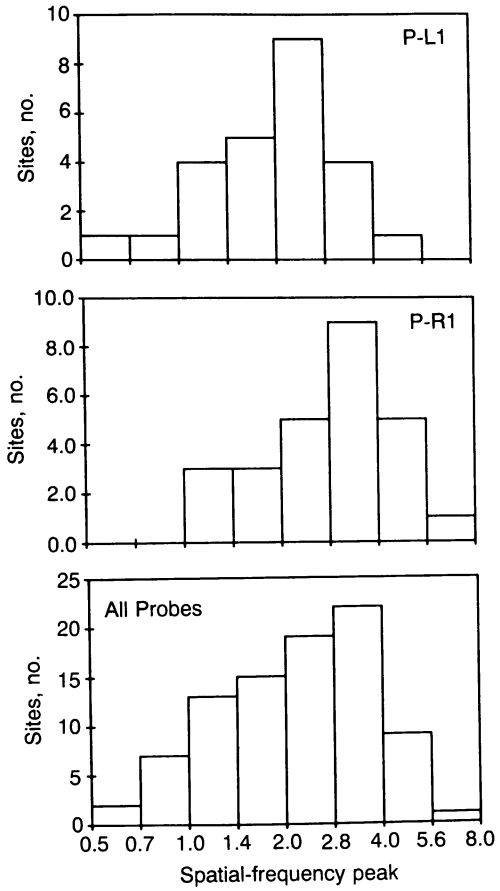

FIG. 2. Histograms of peak spatial-frequency tuning of all cells recorded in various probes. It can be seen that the cells sampled within probes P-L1 (*Top*) and P-R1 (*Middle*) and the total sample (*Bottom*) are distributed over a considerable spatial-frequency range, with most of the cells tuned to mid-spatial-frequencies in unimodal distributions. Special frequency is in c/deg.

population was small and had a highly skewed distribution with tuning preferences covering the entire recorded range. It thus seems more parsimonious to assume that there is a unimodal distribution of cell tuning.

Perhaps the most convincing way to settle the issue of dichotomy versus continuity is to see whether the data are better fit by a bimodal waveform or by some continuous function such as a triangular function. The data are too noisy and sparsely sampled to resolve the shape of the periodic function, but we have found that the data are well fit with a minimum number of free parameters when one assumes an orderly arrangement of spatial-frequency selectivities across the cortex. If the cells are arranged in an orderly progression by spatial frequency, then the space occupied by cells tuned to each spatial-frequency range should be proportional to the number of such cells. As indicated by the histogram, most cells are tuned to midfrequencies, so one would expect the tracks to stay mainly in this range, with brief excursions to high and to low frequencies once per cycle. Fitting this kind of function significantly reduced the squared error ($P < 0.003$) for the most complete probes, indicating that this is a reasonable description of the data. Fits of other periodic functions, such as the sine, square, and triangle waves, with one more free parameter did not significantly improve the fit for either probe. In the light of this result and of the rather strained assumptions one must make to account otherwise for the unimodality of Fig. 2, we can conclude that the spatial-frequency peaks within this cortical region vary systematically.

Correspondence to Histological Markers. The recording data discussed above provide evidence for a continuous, periodic variation in peak spatial-frequency tuning of cells within a tangential strip of cortex. These delineate what we may term "physiological modules." CytOx staining in these portions of the cortex reveals the familiar anatomical modular pattern of CytOx blobs and interblobs. What is the relation between these "physiological modules" and the "anatomical modules"?

We made small electrolytic lesions at two or three points along each of the electrode tracks. With the flattened cortical tissue sectioned almost exactly in the plane of the electrode tracks, most of these markers, along with the CytOx stains, could be seen in a single section. The location of each recording site along the track could then be determined from the lesions. One complication in relating these loci to the CytOx pattern was that the CytOx stain within the region of the track itself was somewhat disturbed, as would be expected. However, there is considerable evidence (12, 15) that the CytOx blobs form a columnar structure through the striate cortex. The blobs and interblobs in sections just below or above the electrode path are thus aligned with those in the sections containing the electrode path itself. Therefore, we quantified the CytOx pattern along the electrode track by densitometric measurements made along the electrode paths in neighboring sections. The tuning properties of cells at each of the recording sites were compared to the density of the CytOx pattern at that location. Fig. 1*A* shows a CytOx-stained section of the left hemisphere. Note the blobs and interblobs and the path of the electrode indicated on the section. Fig. 1*B* shows the CytOx density along this track, and Fig. 1*C* shows the tuning of the cells at corresponding points.

Although the arrangement of the ocular-dominance strips across the striate cortex is generally quite irregular, the strips (and thus the CytOx blobs that lie along the centers of the strips) line up fairly regularly at the V1–V2 border. Here they intersect the representation of the lower vertical meridian of the visual field roughly at right angles. Our electrode penetrations were made approximately at right angles to the V1–V2 border and thus could traverse a single ocular dominance strip. By chance, a probe might go through the center of the strip and thus intersect the blobs, going over the peaks and troughs, so to speak, of blobs and interblobs from one module to the next. But also by chance, a probe might just go down a trough between two rows of blobs and thus stay largely in the interblob regions.

The histological results show that P-R1 traversed interblob regions over much of its extent, whereas P-L1, P-R2, and P-R3 intersected modules closer to the blob centers. The higher average-spatial-frequency tuning of cells in P-R1 than those in the other probes (see Fig. 2) provides physiological evidence consistent with our 2-dG evidence that low-spatial-frequency cells are in the blobs and high-frequency cells are in the interblobs.

More precise evidence comes from relating the actual spatial-frequency tuning at various points along the paths to the CytOx density along the tracks. Fig. 3 presents the results from the three probes with the most extensive data. The CytOx density measures (solid lines) are superimposed on the measures of peak spatial-frequency tuning (dashed lines). In each case, a close relationship can be seen between the density of the CytOx pattern in different regions and the peak tuning of the cells in those regions. Probe L1, for instance, traversed three CytOx blobs and four interblob areas; correspondingly, three troughs and four peaks were found in the peak tuning of cells as a function of distance along the track. The Spearman correlation coefficient between the CytOx density and the peak spatial frequency of the cells was relatively high for each of the four probes: 0.57 ($P < 0.01$), 0.37 ($P < 0.1$), 0.42 ($P < 0.07$), and 0.70 ($P < 0.01$), respectively, for P-L1, P-R1, P-R2, and P-R3.

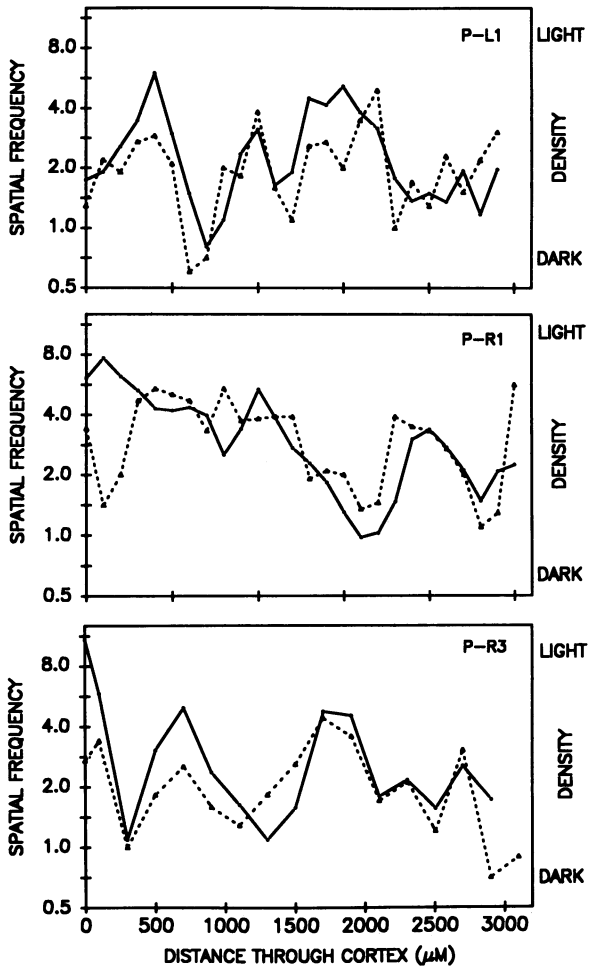

FIG. 3. Comparison for three different probes, of the peak spatial-frequency tuning (••••) of cells with the densitometric values of the CytOx pattern (——) at the corresponding cortical loci. In each case there is good agreement, indicating that the cells tuned to different spatial-frequency ranges are systematically distributed within the cortical modules, in precise correspondence with the CytOx pattern.

One tends to think of blobs and interblobs (or the corresponding stripes and interstripes in V2) as being discrete dichotomous regions. Densitometry of the CytOx pattern across modules does not support this view. It is apparent, for instance, from Fig. 1*B* and the solid lines in Fig. 4 that the density changes from blob to interblob are in fact gradual, not abrupt. (The range over which the densitometric values were smoothed is much smaller than the blobs and does not account for the gradual changes seen.) We have verified this in numerous examinations of the CytOx patterns in regions other than the electrode paths as well. Confirming Horton's initial report (15), we find that the CytOx density changes continuously and gradually from blob centers to interblob regions. From scatter plots (not shown) of CytOx density versus preferred spatial frequency for each track and for the pooled set, which reveal no obvious clusters corresponding to a blob–interblob dichotomy and from Fig. 3, it is clear that the gradual changes in CytOx correspond to the gradual changes seen in the peak spatial-frequency tuning of cells in different parts of a module.

DISCUSSION

Anatomical staining of the striate cortex for CytOx reveals a striking pattern of regions of high CytOx uptake (blobs), interspersed with CytOx-poor areas (interblobs). These Cyt-

Ox blobs serve as very useful anatomical landmarks in what would otherwise be a largely undemarcated expanse of tissue. The fact that the blobs are aligned with the center of the ocular-dominance strips (12, 15, 16) and the spacing between blobs coincides with the dimensions of striate modules gives added importance to these markers.

It has been argued (26) that the division of striate modules into CytOx blobs and interblobs coincides with the location of color-selective vs. luminance-selective cells, respectively, because more color-selective cells were found in the blobs than in interblob regions. Our 2-dG experiments (18, 27), supported by the recording data reported here, lead to quite different conclusions. We found high 2-dG uptake on the blobs with low-spatial-frequency stimuli, whether luminance-varying or color-varying stimuli, and high uptake in the interblobs for high-spatial-frequency stimuli, whether luminance or color. The recording data reported here support this in finding a systematic relation between the spatial-frequency tuning of cells to luminance-varying stimuli and the CytOx pattern. Our color sensitivity is shifted to lower spatiotemporal frequencies with respect to our luminance sensitivity (28), a situation that can be accounted for by the properties of lateral geniculate cells (29). Thus, if color and luminance cells are located in register on the basis of their spatial-frequency tuning, one would expect to find relatively more color-selective cells in the blobs and relatively more luminance-selective cells in the interblobs just by virtue of the differential spatial-frequency tuning of the color and luminance systems.

The evidence presented here also raises the question of whether the blob–interblob pattern actually reflects a functional dichotomy or not. There is much reason to believe that there is a continuum of spatial-frequency tuning among striate cells and a continuum of spatial-frequency channels underlying our spatial vision. Furthermore, our measures of the CytOx pattern show a continuous density variation from the center out, not a blob–interblob dichotomy. This suggests (*i*) that the apparent dichotomy seen in the 2-dG uptake results from the limited spatial resolution of this procedure and (*ii*) that there is in fact a continuum of peak tuning of cells within a module in correspondence with a continuum of CytOx density. The modular organization appears to be a radial pattern, with cells tuned to the lowest spatial frequencies in the center of the blobs and those tuned to increasingly higher frequencies in rings around this center.

If the blobs and the interblobs projected to different prestriate areas, this would provide evidence for their representing a functional dichotomy. However, while blobs and interblobs project to the thin stripes and interstripes of V2, respectively (30, 31), both of these subregions project to V4 (32, 33). Thus, while cells with different spatial tuning are kept in discrete locations through at least V2, one need not conclude that the blob–interblob pattern indicates a dichotomous functional split of the visual information.

It is not known why some areas of V1 and V2 have more CytOx than others. However, as might well be expected from this metabolic enzyme, CytOx density appears to be influenced by the long-term activity rate of the cells involved. For instance, the blobs related to one eye weaken within 10 days of enucleation of that eye (12, 15). The correlation we find between CytOx density and spatial-frequency tuning may just reflect the extent to which cells tuned to various spatial-frequency ranges are stimulated by stimuli in the natural environment: in almost any visual scene, the power drops off systematically from low to high spatial frequencies (34), so low-spatial-frequency cells would be expected chronically to receive more stimulation [if cells tuned to various ranges had equal octave bandwidths, their relative stimulation would perhaps be uniform, but low-spatial-frequency cells in fact have broader spatial frequency and orientation bandwidths than those tuned to high spatial frequencies (5)].

We have argued that cortical modules are organized by ocular dominance and tuning to different two-dimensional spatial frequencies. Regardless of whether or not one feels comfortable in modeling striate cortex receptive fields as quasi-linear two-dimensional spatial-frequency filters, the spatial-frequency tuning of striate cells is evidently a marker for position within a module relative to the center of the CytOx blobs. As such it may guide anatomical studies of the microcircuitry of V1 and of CytOx-rich vs. CytOx-poor domains within V1, and possibly within V2 as well.

We are grateful for the very helpful comments on an earlier version of this manuscript by Martin S. Banks, Kenneth Nakayama, and Eugene Switkes. This work was supported by Public Health Service Grants EY-00014 and AGO-5681, and National Science Foundation Grant BNS 85-19613.

1. Hubel, D. H. & Wiesel, T. N. (1962) *J. Physiol. (London)* **160,** 106–154.
2. Maffei, L. & Fiorentini, A. (1973) *Vision Res.* **13,** 1255–1267.
3. Movshon, J. A., Thompson, I. D. & Tolhurst, D. J. (1978) *J. Physiol. (London)* **283,** 101–120.
4. De Valois, R. L., Yund, E. W. & Hepler, N. (1982) *Vision Res.* **22,** 531–544.
5. De Valois, R. L., Albrecht, D. G. & Thorell, L. G. (1982) *Vision Res.* **22,** 545–559.
6. Campbell, F. W. & Robson, J. G. (1968) *J. Physiol. (London)* **197,** 551–566.
7. Blakemore, C. & Campbell, F. W. (1969) *J. Physiol. (London)* **203,** 237–260.
8. Kelly, D. H. (1976) *Vision Res.* **16,** 277–287.
9. De Valois, R. L. & De Valois, K. K. (1988) *Spatial Vision* (Oxford Univ. Press, New York).
10. Hubel, D. H. & Wiesel, T. N. (1974) *J. Comp. Neurol.* **158,** 267–294.
11. Hubel, D. H. & Wiesel, T. N. (1977) *Proc. R. Soc. London Ser. B* **198,** 1–59.
12. Horton, J. C. & Hubel, D. H. (1981) *Nature (London)* **292,** 762–764.
13. Humphrey, A. L. & Hendrickson, A. E. (1983) *J. Neurosci.* **3,** 345–358.
14. Tootell, R. B. H., Silverman, M. S., De Valois, R. L. & Jacobs, G. H. (1983) *Science* **220,** 737–739.
15. Horton, J. C. (1984) *Philos. Trans. R. Soc. London Ser. B* **304,** 199–253.
16. Switkes, E., Tootell, R. B. H., Silverman, M. S. & De Valois, R. L. (1986) *J. Neurosci. Methods* **15,** 269–280.
17. Tootell, R. B. H., Silverman, M. S., Switkes, E. & De Valois, R. L. (1982) *Soc. Neurosci. Abstr.* **8,** 707.
18. Tootell, R. B. H., Silverman, M. S., Hamilton, S. L., Switkes, E. & De Valois, R. L. (1988) *J. Neurosci.* **8,** 1610–1624.
19. Tootell, R. B. H., Hamilton, S. L., Silverman, M. S. & Switkes, E. (1988) *J. Neurosci.* **8,** 1500–1530.
20. Tootell, R. B. H. & Silverman, M. S. (1985) *J. Neurosci. Methods* **15,** 177–190.
21. Silverman, M. S. & Tootell, R. B. H. (1987) *J. Neurosci. Methods* **19,** 1–10.
22. Tootell, R. B. H., Silverman, M. S., Switkes, E. & De Valois, R. L. (1982) *Science* **218,** 902–904.
23. Fisher, R. A. (1929) *Proc. R. Soc. Ser. A* **125,** 54–59.
24. Whittle, P. (1952) *Trab. Estad.* **3,** 45–57.
25. Klein, S. A. & Levi, D. M. (1985) *J. Opt. Soc. Am. Sect. A* **2,** 1170–1190.
26. Livingstone, M. S. & Hubel, D. H. (1984) *J. Neurosci.* **4,** 309–356.
27. Tootell, R. B. H., Silverman, M. S., Hamilton, S. L., De Valois, R. L. & Switkes, E. (1988) *J. Neurosci.* **8,** 1569–1593.
28. van der Horst, G. J. C. & Bouman, M. A. (1969) *J. Opt. Soc. Am.* **59,** 1482–1488.
29. De Valois, R. L. & De Valois, K. K. (1975) in *Handbook of Perception*, eds. Carterette, E. C. & Friedman, M. P. (Academic, New York), Vol. 5, pp. 117–166.
30. Livingstone, M. S. & Hubel, D. H. (1983) *Nature (London)* **304,** 531–534.
31. De Yoe, E. A. & Van Essen, D. C. (1985) *Nature (London)* **317,** 58–61.
32. Shipp, S. & Zeki, S. (1985) *Nature (London)* **315,** 322–325.
33. De Yoe, E. A., Felleman, D. J., Krienin, J. J., Olavaria, J. & Van Essen, D. C. (1988) *Invest. Ophthal. Vis. Sci.* **29,** 115.
34. Field, D. J. (1987) *J. Opt. Soc. Am. Sect. A* **4,** 2379–2394.